

PLOS Water

Contemporary and Relic Waters Strongly Decoupled in Arid Alpine Environments

Brendan J. Moran (ORCID = 0000-0002-9862-6241)¹, David F. Boutt (ORCID = 0000-0003-1397-0279)¹, Lee Ann Munk (ORCID = 0000-0003-2850-545X)², Joshua D. Fisher^{3,4} (ORCID = 0000-0003-1054-3132)

¹ Department of Earth, Geographic, and Climate Sciences, University of Massachusetts-Amherst, Amherst, MA, USA

² Department of Geological Sciences, 3101 Science Circle, University of Alaska-Anchorage, Anchorage, AK, USA

³ Advanced Consortium on Cooperation, Conflict, and Complexity, Earth Institute, Columbia University, New York, NY, USA

⁴ Network for Education and Research on Peace and Sustainability, Hiroshima University, Higashihiroshima, Japan

Corresponding author: Brendan J. Moran (bmoran@umass.edu)

46 **Abstract**

47 Deciphering the dominant controls on interconnections between groundwater, surface
48 water, and climate is critical to understanding water cycles in arid environments, yet persistent
49 uncertainties in the fundamental hydrology of these systems remain. The growing demand for
50 critical minerals such as lithium and associated water demands in these arid environments has
51 amplified the urgency to address these uncertainties. We present an integrated hydrological
52 analysis of the Dry Andes region utilizing a uniquely comprehensive set of tracer data (^3H ,
53 $^{18}\text{O}/^2\text{H}$) for this type of environment, paired directly with physical hydrological observations. We
54 find two strongly decoupled hydrological systems that interact only under specific
55 hydrogeological conditions where preferential conduits have developed. The primary conditions
56 in these conduits form are when laterally extensive fine-grained evaporite and/or lacustrine units
57 or perennial flowing streams exist in connection with groundwater discharge sites. These
58 conduits which efficiently capture and transport modern or “contemporary” water (weeks to
59 years old) within the system control the interplay between modern hydroclimate variations and
60 groundwater aquifers. Modern waters account for a small portion of basin budgets but are critical
61 to sustaining surface waters due to the existence of these conduits. As a result, surface waters
62 near basin floors are disproportionately sensitive to short-term climate and anthropogenic
63 perturbations. This framework describes a new understanding of the dominant controls on
64 natural water cycles intrinsic to these arid high-elevation systems which improves our ability to
65 manage critical water resources.

66 **1. Introduction**

67 Water is a scarce but essential resource for human societies and ecosystems in Earth’s driest
68 regions (Gleeson et al., 2020). Due to the nature of water cycles and hydrogeological systems in

69 these environments, groundwater is an especially critical freshwater resource for both humans
70 and ecosystems (Bierkens & Wada, 2019; Immerzeel et al., 2020). This is particularly true of
71 arid, high-elevation regions where steep gradients in topography and climate develop deep water
72 tables and long transit times leading to the increased importance of multi-decadal groundwater
73 storage in water budgets (Haitjema and Mitchell-Bruker 2005; Gleeson et al. 2011). In many of
74 these regions direct (i.e. water extraction) and indirect (i.e. global climate change) anthropogenic
75 impacts are increasing and threatening the quantity and quality of both groundwater and surface
76 water (Wang et al., 2018; Zipper et al., 2020). The resulting relative and in some cases absolute
77 scarcity can increase social tension among riparian parties including communities, governmental
78 authorities, and industry users (Mehran et al., 2017; Mehran et al., 2015; AghaKouchak et al.,
79 2015). In addition, responses to natural perturbations (i.e. droughts) are often not well
80 understood in these environments (Gleeson et al., 2012; Ashraf et al., 2021) making sustainable
81 and equitable water management challenging. In arid, remote regions, limited precipitation and
82 the importance of basin-scale groundwater flow systems together with a lack of long-term, high-
83 quality instrumental records make responsibly allocating water resources challenging (Somers &
84 McKenzie, 2020; Moran et al., 2022). These conditions also mean that surface water is scarce
85 and groundwater discharge sourced from relic water (100s to 1000s of years old) often underpins
86 the hydrological cycle, acting as critical buffers to hydrological systems from large inter-annual
87 fluctuations (Fan et al., 2013; Bierkens & Wada, 2019; Mcknight et al., 2023). Fundamental
88 questions remain to be answered about the hydrological functioning of these systems
89 perpetuating persistent uncertainties around water sources and transport in these environments.
90 This raises important questions about water scarcity issues in the face of increasing water
91 resource development and the likely consequences of global climate change.

92 The Dry Andes of South America, marked by one of Earth’s highest and broadest
93 plateaus on the margin of the driest nonpolar desert, is one of the most extreme places on the
94 planet (Hartley & Chong, 2002; Rech et al., 2019). This region is often referred to as the
95 “Lithium Triangle” as it holds a majority of the world’s reserves of the battery component metal
96 in the form of Li-bearing brines under its salt flats or “Salares” (Munk et al., 2016). The
97 exploitation of this resource has rapidly expanded in the push to decarbonize the global
98 economy, highlighting concerns over the sustainability of intensive groundwater extraction
99 (Gajardo & Redón, 2019; Gutiérrez et al., 2018; Sonter et al., 2020), equitable water
100 management, and the tradeoffs of water allocation and water management decisions (Crawford et
101 al., 2021; Diaz Paz, et al. 2023). This landscape is composed of many adjoining endorheic basins
102 with hyper-arid to arid conditions (<50 mm of precipitation/year) on their basin floors where
103 groundwater recharge occurs primarily at the highest elevations near watershed divides
104 (Houston, 2002, 2007, 2009; Boutt et al., 2021). Thick vadose zones (>100 m) across nearly the
105 entire landscape and intense solar insolation create conditions where actual groundwater
106 recharge and evaporation rates are difficult to quantify and sources of water difficult to trace
107 (Rissmann et al. 2015; Scheihing et al. 2018; Viguiet et al. 2020). Where water tables reach the
108 surface near basin floors, large evaporite deposits, and persistent saline water bodies have
109 formed (Corenthal et al., 2016; Munk et al., 2021). Persistent surface water features
110 (saline/brackish lagoons, vegetated wetlands, and perennial and intermittent streams) and their
111 interconnections are controlled by a combination of lithology, topography, and structure, yet
112 deciphering the specific controls on connectivity between these features, the modern
113 hydroclimate and regional groundwater remains elusive (Munk et al., 2021). In addition,
114 paleoclimate records indicate that at least four major pluvial periods have occurred over the past

115 ~100 ka, increasing precipitation by a factor of 2-3 times modern rates (Gayo et al. 2012;
116 Placzek et al. 2013). These wet periods dramatically altered the hydrological and ecological
117 conditions (Pfeiffer et al., 2018), and the effects are likely still evident in the modern
118 hydrological system in the form of transient groundwater storage changes within the deep and
119 extensive regional aquifers responding over 100-10,000-year time scales (Moran et al., 2019).
120 These conditions have accentuated distinctions between the regional groundwater system and
121 surface waters, making it an ideal testing ground to address these persistent questions in arid
122 hydrology.

123 The challenge of hydrological budget closure in these environments has been well
124 documented worldwide and highlights the uncertainties that remain to be addressed (van Beek et
125 al. 2011; Liu et al., 2020; Boutt et al., 2021). Imbalances where calculated inflows are smaller
126 than outflows are observed in nearly every arid region worldwide (Belcher et al., 2009; Ge et al.,
127 2016; Wood et al., 2015; Kröpelin et al., 2008; Wheatler et al., 2007), including in the massive
128 Salar de Atacama basin on the western edge of the Andean plateau (Corenthal et al., 2016; Munk
129 et al., 2018). Major unresolved questions include groundwater transit time characteristics,
130 surface water sources and residence times, and interconnectivity between groundwater, surface
131 hydrology, and climate (Favreau et al., 2009; Gleeson et al., 2011; Walvoord et al., 2002).
132 Recent work in the basins of the Dry Andes has shown that true hydrological catchments often
133 cross topography and include substantial inputs from relic groundwater sourced from long-flow
134 paths and/or groundwater storage head-decay (Jordan et al., 2015; Corenthal et al., 2016; Moran
135 et al., 2019). Therefore, modern water budgets do not come close to closure at steady-state with
136 modern climate inputs (Boutt et al., 2021). Though the inputs from modern precipitation are
137 relatively small, large infrequent precipitation events play an important role in sustaining salar

138 floor water bodies in these environments through preferential recharge and areas of restricted
139 vertical infiltration (Boutt et al., 2016; Munk et al., 2021). Other work shows the critical role that
140 evaporite stratigraphy has on the expression of surface water features and their connection to
141 modern precipitation inputs and groundwater discharge (Mcknight et al., 2021; Munk et al.,
142 2021). Recent work by Moran et al., (2022) establishes that modern water accounts for a
143 relatively small portion of water budgets but is critical to sustaining surface water bodies and
144 wetlands, as a result, these arid systems are uniquely sensitive to climate (drought) and
145 anthropogenic perturbations on short time scales. Much of this work has been focused on the
146 western edge of the Dry Andes, while other work has explored these issues in basins further east
147 (Godfrey et al., 2013; Gamboa et al., 2019; Frau et al., 2021) but a mechanistic framework to
148 explain our observations region-wide has not been established.

149 Substantial gaps remain in our understanding of the time scales and spatial definition of
150 primary interconnections that constitute water cycles in these environments, specifically the
151 controls on groundwater, surface water, and modern climate interactions (Masbruch et al., 2016).
152 We investigate these remaining uncertainties using a large dataset of tritium activity in water
153 paired with stable oxygen and hydrogen isotope signatures, and hydrophysical and
154 hydrogeochemical field observations. Utilizing a new approach to integrating and interpreting
155 the well-established systematics of these tracers we present a process-based conceptual
156 framework that describes two dominant archetypes of flow systems in these environments and
157 the controls on connections between their constituent parts. This new framework provides
158 critical insight into expected responses to perturbations (natural and anthropogenic) in the Dry
159 Andes and describes intrinsic hydrological processes for arid alpine systems worldwide.

160 **2. Methods**

161 **2.1. Water sample analysis**

162 To assess spatially explicit water residence times within these hydrological systems we
163 utilize stable ($\delta^{18}\text{O}$ & $\delta^2\text{H}$) and radiogenic (^3H) isotopic tracer measurements in 142 water
164 samples collected across the Dry Andes. These include surface and groundwaters collected
165 during numerous field campaigns between October 2011 and March 2021 in Salar de Atacama
166 (data first presented in Moran et al. 2022) and from 2019 and 2020 on the Puna Plateau. Samples
167 were collected with a consistent, standardized procedure and in-situ measurements of
168 temperature, specific conductance, and pH were made at each sampling location during
169 collection. Tritium activity in water samples was measured at the Dissolved and Noble Gas
170 Laboratory, University of Utah. Samples were collected in 1 L HDPE bottles with minimal
171 headspace. In the lab, 0.5 L aliquots were distilled to remove dissolved solids. These water
172 samples were then degassed in stainless steel flasks until $<0.01\%$ of dissolved gas remained and
173 sealed to ingrow helium. ^3H concentrations were measured by helium ingrowth (Clarke et al.,
174 1976); 6–12 weeks is typically adequate to ingrow sufficient ^3He from the decay of ^3H ($t^{1/2} =$
175 12.32 yr.; Lucas & Unterweger, 2000) for analysis. ^3He concentrations were then measured on a
176 MAP215-50 magnetic sector mass spectrometer using an electron multiplier to measure low
177 abundance ^3He , which was directly correlated with the amount of ^3H decayed. Data are reported
178 in tritium units (TU) on the date of sampling, where one TU is equivalent to one tritium atom per
179 10^{18} hydrogen atoms ($^3\text{H}/\text{H} \cdot 10^{18}$) (Kendall & Caldwell, 1998). Several duplicate analyses of the
180 same sample were conducted to confirm important values, and the reproducibility for these
181 samples is of the same order as the precision of the measurement. The analytical error associated
182 with each sample is reported along with the full dataset in the supplemental material.

183 Water samples were analyzed for $\delta^2\text{H}$ and $\delta^{18}\text{O}$ using wave-length scanned cavity ring-
184 down spectroscopy (Picarro L-1102i); samples were vaporized at 120°C (150°C for higher salt
185 content waters) in the Stable Isotope Laboratory at the University of Alaska Anchorage.
186 International reference standards (IAEA, Vienna, Austria) were used to calibrate the instrument
187 to the VSMOW-VSLAP scale and working standards (USGS45: $\delta^2\text{H} = -10.3\text{‰}$, $\delta^{18}\text{O} = -2.24\text{‰}$
188 and USGS46: $\delta^2\text{H} = -235.8\text{‰}$, $\delta^{18}\text{O} = -29.8\text{‰}$) were used with each analytical run to correct for
189 instrumental drift. Long-term mean and standard deviation records of a purified water laboratory
190 internal QA/QC standard ($\delta^2\text{H} = -149.80\text{‰}$, $\delta^{18}\text{O} = -19.68\text{‰}$) yield an instrumental precision of
191 0.93‰ for $\delta^2\text{H}$ and 0.08‰ for $\delta^{18}\text{O}$. The full dataset is provided in the supplemental material.

192 **2.2. Tritium Age Tracing Approach**

193 The hydrological system in this region is complex and heterogeneous on all scales, and
194 large gaps exist in hydrogeological and hydroclimatological data coverage, especially above the
195 basin floors at the higher elevation plateaus and mountain peaks. Very deep water tables (100s of
196 meters) and rugged terrain make direct observation of the groundwater system impractical across
197 much of the landscape. Long-term high-quality terrestrial monitoring of climatology and
198 streamflow flow is also sparse. Therefore, highly parameterized models and tracers that require
199 additional assumptions are not the most effective tools to assess water flux rates or transit times
200 in this environment. Tracing signatures recorded in the water molecule itself most reliably
201 integrate small-scale variability with large-scale processes and can be captured with individual
202 water samples (Birkel et al., 2015; Buttle, 1994). Stable isotope ratios ($\delta^{18}\text{O}$, $\delta^2\text{H}$) and
203 radioisotopes (^3H) in water offer many unique advantages in these systems (Cook & Bohlke,
204 2000; Kendall & Caldwell, 1998). Besides the well-understood influence (fractionation) from
205 low and high-temperature water-rock interaction and evaporation, signatures of $\delta^{18}\text{O}$ & $\delta^2\text{H}$ in

206 groundwater recharge remain unchanged from infiltration until re-emergence from the ground
207 (Beria et al., 2018; Clark & Fritz, 1997; Kendall & McDonnell, 1998). Geothermal water-rock
208 interactions cause a pronounced “oxygen shift” in $\delta^{18}\text{O}$ & $\delta^2\text{H}$ cross-plot space and a trend line
209 with a slope approaching zero (Panichi and Gonfiantini, 1977). Evaporation causes the signature
210 of a water parcel to increase in deuterium-excess and deviate from the GMWL along a steep,
211 positive linear slope. Deuterium excess (d-excess) is the deviation from the global meteoric water
212 line defined as $\text{d-excess} = \delta^2\text{H} - 8 * \delta^{18}\text{O}$ (Dansgaard, 1964). These fractionation processes both
213 act to progressively increase the d-excess value in a sample or group of samples but can be
214 reliably differentiated from each other through comparison of the slopes of the apparent local
215 evaporation line trends (LEL) defining groups of samples (Rissmann et al., 2015, Moran et al.,
216 2019).

217 Radioisotope signatures (^3H) are also conservative but follow a predictable decay (half-
218 life of 12.32 years) during transit. To effectively utilize this tracer, we must constrain the ^3H
219 content of modern precipitation, this defines the signature of direct modern inputs to the
220 hydrologic system. Widespread atmospheric nuclear bomb testing in the late 1950s and early
221 '60s created a large and unmistakable peak in global atmospheric ^3H concentrations which
222 increased activities in precipitation globally by greater than an order of magnitude (Cartwright et
223 al., 2017). We assume the modern value in precipitation described above is representative of
224 average precipitation from about 2000 to the present since the bomb peak signature is no longer
225 resolvable after that date in the Southern Hemisphere (Rooyen et al., 2021). This modern
226 signature is also representative of precipitation before the mid-1950s since the bomb peak had
227 not yet occurred (Houston, 2007; Jasechko, 2016). This period of high ^3H activity in
228 precipitation and therefore in recharge during that time allows for reliable differentiation

229 between water recharged post-1955 and that before 1955 because if this strong signature is not
230 observed in water (very low ^3H activity), very little if any of that water is composed of recharge
231 after the bomb peak. Since the ^3H activity in any given sample is a bulk sample representing
232 mixtures of unknown sources and respective amounts, we must also be careful not to over-
233 interpret specific ^3H activities in individual samples without proper physical constraints.
234 Therefore, to ensure a reliable and conservative interpretation of this broad dataset we determine
235 a simple “percent modern water” ratio in each sample as the ratio of modern precipitation input
236 activity to the activity measured in the sample. Using the ^3H activity in modern precipitation, we
237 determine the proportion of modern or “contemporary” and pre-modern or “relic” water
238 components in the sample according to the formula: *Percent Modern Water in Sample* =
239
$$\frac{{}^3\text{H Activity in Sample}}{{}^3\text{H Activity in Modern Precipitation}}$$

240 The ^3H activities in modern precipitation over the region, also presented by Boutt et al.
241 (2016) and Moran et al. (2019), are determined to be 3.17 ± 0.53 TU from 5 amount-weighted
242 rain and snow samples collected between 2013 and 2014 in the western part of the region
243 (Chile); and determined to be 4.54 ± 1.34 TU from 3 amount-weighted rain and snow samples
244 collected between 2018 and 2019 in the eastern region (Argentine Puna) (**Figure 1**). These
245 values are within the range reported by others in the region (Cortecci et al., 2005; Grosjean et al.,
246 1995; Herrera et al., 2016; Houston, 2002, 2007). Consistent with other studies in this region and

Figure 1. Surface and groundwaters in the Dry Andes analyzed for ^3H , $\delta^{18}\text{O}$, and $\delta^2\text{H}$ in this study (n=142). Pie charts represent percent modern content, colored outlines show general water type groupings and colored dots show sample sites and their physical water type. The black crosses are precipitation sample sites used in ^3H analysis. Black outlines show internally drained basins, blue solid lines are perennial streams, and blue dashed lines are intermittent streams. Important features (salars, mountains, rivers) are noted along with their elevations. (a) Map of the Salar de Atacama basin and the northern Puna region to the east, where pie charts represent average content of inflow zones and surface waters in order to display all data (see Moran et al., 2022). (b) Map of the southern Puna where each pie chart represents one sample. (c) A schematic cross-section of salar-basin floor hydrogeological systems describing the physical water classifications.

247 across the southern hemisphere, the ^3H activities in precipitation have now stabilized to reflect
248 modern production and so this value accurately reflects (within uncertainty) any recharge that
249 occurred within the last few decades (Basaldúa et al., 2022). Water recharged in 1955 before the
250 bomb peak with a ^3H activity of 3.17 ± 0.53 TU would have between 0.07 and 0.10 TU in June
251 2020, or about 2-3% of the modern precipitation input; water with a ^3H activity of 4.54 ± 1.34
252 TU would have between 0.08 and 0.15 TU in June 2020, also about 2-3% of the modern
253 precipitation input (Stewart et al., 2017). Due to the small but non-negligible analytical
254 uncertainty (~ 0.02 - 0.07 TU at low activities), samples with these very small activities are herein
255 considered to be effectively ^3H -dead waters or indistinguishable from zero. Waters registering
256 such low activities are assumed to contain negligible volumes of water recharged post-bomb
257 peak (1955), as even small amounts of water with these higher activities would heavily skew
258 resultant activities in these ^3H -dead samples to appear to contain high levels of modern water.
259 Since most of the waters measured in this environment contain effectively no ^3H , our objective is
260 not to directly estimate discrete mean residence time distributions but instead to describe the
261 relative proportions of ^3H -dead to recent recharge (<65 years old) in these waters (Cartwright et
262 al., 2017). This relative water age value allows for the reliable interpretation of connections to
263 modern precipitation inputs, as well as the lack thereof.

264 **3. Results & Discussion**

265 **3.1. Physical water-type groupings**

266 Sampled waters were grouped into seven physical water types. These distinctions are
267 based on extensive knowledge of the regional hydrogeology gathered during more than ten field
268 campaigns in Salar de Atacama on the Puna Plateau, previously published works, and scrutiny of
269 geochemical signatures (Munk et al., 2021). A schematic cross-section describing these water

270 groupings is shown in **Figure 1c**. Nucleus Brines are groundwaters from the core of the halite-
271 dominated brine aquifer, sampled at shallow depths <13 meters below ground level (mbgl),
272 Marginal Brines are groundwaters from the margins of the brine aquifer, sampled at the water
273 table (<2 mbgl). Transitional Pools are highly saline, shallow pools that form at the margin of the
274 halite crust that grow and shrink rapidly primarily in response to precipitation events. These are
275 often adjacent to (~1-2km away) but distinct from the Lagoons (saline lakes). Many of these
276 Lagoon water bodies also grow and shrink seasonally and after precipitation events but are
277 perennially extant. They are also quite shallow (<1m) but much less saline than the Transitional
278 Pools. In Salar de Atacama we were able to access groundwater wells, whereas, in the Puna
279 region, these brine bodies are present in the vicinity of the salars indicated in **Figure 1**, there are
280 currently very few accessible groundwater wells that could be sampled. In addition, on the high-
281 elevation plateau, there are no true Transitional Pools as there are in Salar de Atacama. The
282 waters classified as “inflows” are separated into three groups; Streams are perennially and
283 intermittently flowing fresh surface waters, Inflow Groundwaters (Inflow Gw) are fresh to
284 brackish waters sampled from wells and from persistent springs that we define as groundwater
285 outcrops, and Transition Zone Groundwaters are brackish to saline waters sampled at the water
286 table within the transition zone between the inflow water bodies and the brines.

287 **3.2. Water transit time partitioning**

288 We assess tritium (^3H) activities in 142 samples representing all major physical water
289 types covering a large swath of the Dry Andes. In this environment where modern water and pre-
290 modern water appear to be strongly decoupled in terms of where they exist on the landscape,
291 determining the relative proportion of each in a sample is a highly effective way to define the
292 relative transit age and therefore sources of water to different water bodies. A detailed summary

293 of this analysis and the raw and derived data presented in the results is provided in the
294 supplemental material (**Table S1**).

295 The geographical distribution of relative water age across the region highlights important
296 results concerning surface and groundwater on basin floors and inflow waters to the basins
297 (**Figure 1**). First, in the Salar de Atacama basin, all basin inflow waters (streams, springs, and
298 groundwaters) are principally composed of pre-modern water (ie. 0-5% modern; Moran et al.,
299 2022). Relative modern water components in inflow waters are consistent across several years,
300 and in different seasons of site repeat sampling, larger river waters show higher seasonal and
301 yearly variability due to their direct and more rapid interaction with modern precipitation inputs
302 (**Figure S1**). Waters at the basin floor, in saline surface waters, and brine groundwaters also
303 show consistently larger components of modern water. In addition, two high-elevation (4100
304 masl) fresh-to-brackish lakes near the watershed divide contain ~30% modern water, similar to
305 the basin floor surface waters. These results demonstrate the strong distinctions that exist
306 between overall inputs to these basin water budgets and the near-surface waters at the basin
307 floors, especially since recent inflow waters are critical to sustaining these surface waters. These
308 general observations also describe the higher-elevation plateau endorheic basins to the east.
309 Inflow groundwaters, which here consist of spring complexes that are effectively “outcrops” of
310 and discharge from the groundwater system to the surface, have very low modern water content
311 (0-2%). Basin floor waters on the plateau (saline surface waters) also have substantially higher
312 modern water content than the nearby groundwaters.

313 There are a few important distinctions between water age distributions on the plateau and
314 at the lower elevation of Salar de Atacama. One is that many of these higher elevation basin floor
315 waters (brackish-brine lagoons) have modern water contents of >50%, some of the highest values

316 observed in the region. Two exceptions to this are the lagoons at Salar del Hombre Muerto and
317 Salar del Carachi Pampa. Another key distinction is the consistently high modern water content
318 in streams on the Puna plateau, particularly in the large perennial rivers of Rio Los Patos and Rio
319 Punilla which average ~22% modern, and streams in the northern Puna region which average
320 46%. The vegetated wetland complexes above the basin floors, common to the high elevations of
321 this region, have consistently higher modern water content than nearby groundwaters and
322 streams. The commonalities in transit age across the whole region and the distinctions between
323 low-elevation and high-elevation systems are valuable in deciphering the dominant controls on
324 water transport and interconnectivity.

325 Examining the distribution of these data across the region allows for further examination
326 of common dominant controlling mechanisms across the many individual basin systems.
327 Kruskal-Wallis tests were conducted on data groupings in each panel of **Figure 2** showing that
328 the groupings chosen are statistically unique (P-value <0.001) except when grouped by Sample
329 Elevation Above Basin Floor (P-value=0.09), detailed results of these tests are provided in the
330 supplemental material (**Table S2**). **Figure 2a** shows the distribution of the water age ratios
331 grouped by water type, a definition based on the position between recharge and discharge zone,
332 and salinity (described schematically in **Figure 1c**). Inflow groundwaters average <5% modern
333 water content, similar to stream waters yet stream data skew towards very low modern water
334 values. Importantly several stream samples show higher modern water content of between 15%
335 and 60%, these samples are of the large perennial streams mentioned above. Saline surface

Figure 2. Statistical distributions of ³H-derived percent modern water results. Grey boxes inside the polygons show the interquartile range; red dots are the median and polygons represent the frequency distribution of the data (black dots). Data grouped by (a) physical water type, where colors of polygons correspond to physical water type dots in Figure 1; (b) by elevation of sample; (c) by specific conductance of sample, where colors of polygons show fresh (blue) to brine (pink) waters; and (d) by sample elevation above the basin floor (basin floor elevations indicated in Figure 1).

336 waters near the basin floors average 20-30% modern while the lagoons (perennial saline lakes) in
337 particular show a large range in values but also skew towards the lower values. The brine
338 groundwater bodies within the salar evaporites and the brackish groundwaters in the transition
339 zone between fresh inflow and brine (TZ Gw) show two primary groupings of relative age. One
340 of very low modern water content and the other close to 25% modern, this younger water
341 component is most clearly shown in the marginal brine waters but is also present in the other two
342 water bodies. Grouped by sample elevation we observe that on average, more modern water
343 exists near the surface above 3000 masl but also that waters with very small modern components
344 are present at all elevations (**Figure 2b**). Importantly the lowest elevations show clusters of
345 samples with modern content similar to the highest elevations. These characteristics can also be
346 seen when grouped by elevation above the basin floor (**Figure 2d**), where samples collected
347 highest above the basin floor average higher modern water content. Most samples were collected
348 very near basin floors, which reflects the concentration of near-surface water and its absence
349 elsewhere, and shows a wide distribution of water ages. Grouped by specific conductivity (a
350 proxy for salinity) we see that the freshest water is predominately relic but also that there are
351 many freshwaters with much higher modern content. Average water age generally increases with
352 salinity but the saltiest waters (brines) also contain a range of ages from <3% modern to nearly
353 95% modern. These results provide many important insights into where pre-modern and modern
354 water persist in this system, their sources, and how they interact.

355 These results highlight the strong influence of hydroclimate, topography, and
356 hydrogeology on transit time and interaction with modern inputs. In this arid environment,
357 modern water is not spatially common but differences in climate across the region have
358 important influences on surface hydrology. Region-wide, groundwaters, and most streams have

359 very small modern components reflecting the long transit times from their source waters. But the
360 large perennially flowing streams that exist at the colder and slightly wetter climate at these
361 higher elevations, have a substantial portion of their flow composed of modern water. Vegetated
362 wetland complexes or vegas can be extensive and often form near basin floors at the periphery of
363 salars, high elevation wetlands or peatlands referred to in this region as bofedales also occur
364 sporadically on the Puna above 3800 masl around groundwater outcrops or springs (Marconi et
365 al., 2022). Although these two systems are characterized by different ecology, they display
366 similar hydrological characteristics in that they are strongly influenced by recent precipitation
367 inputs; we refer to all these systems together herein as vegas. The consistently strong signature in
368 surface water bodies at basin floors exists across the region but the climate at higher elevations
369 appears to create conditions where less than half of their water is composed of regional
370 groundwater. Specific hydrogeological and ecological conditions that allow water tables to
371 persist close to the surface (<5m) are a shared feature of all of the water bodies mentioned above.
372 We argue that these conditions strongly control how modern water enters and moves through this
373 system since most precipitation either evaporates in the thick vadose zones or slowly infiltrates
374 towards the groundwater table below.

375 **3.3. Hydrogeological mechanisms controlling source partitioning**

376 We further investigate mechanisms controlling the partitioning of waters in this
377 environment using d-excess signatures paired with percent modern water content (**Figure 3a**).

Figure 3. (a) Processes controlling physical water distinctions and interactions based on ^3H , $\delta^{18}\text{O}$, and $\delta^2\text{H}$ signatures. Circles are proportional to the average magnitude of discharge at each stream site, SdA streams plot within the black dashed box. The grey vertical bar is the Global Meteoric Water Line (GMWL), and the blue box at the top represents the approximate range of meteoric input waters in the region (based on Moran et al., 2019 data). Arrows depict the influence of important hydrological processes and interactions. (b) Shows these data plotted in $\delta^{18}\text{O}$ - $\delta^2\text{H}$ space relative to the LMWL (Rissmann et al. 2015) and evaporation trends of basin floor waters in Salar de Atacama and on the higher elevation Puna plateau.

378 The δ -excess provides a reliable measure of the amount of evaporation a sampled water has
379 undergone, placing important constraints on waters that have had little or no atmospheric
380 interaction from that which has undergone substantial evaporation (waters with increasing
381 negative values). We group all stream samples by average streamflow at the sample site to
382 highlight the relative size of each stream and therefore the relative volume of modern water
383 represented by the ratio (data provided in **Tables S3**).

384 The inflow groundwaters plot close to the Global Meteoric Water Line (GMWL) as they
385 are composed of infiltration that interacted minimally with the atmosphere before becoming
386 groundwater, and their modern water content indicates nearly all of their volume is composed of
387 relic water. The streams also plot along the GMWL and most have similar mean age profiles to
388 the inflow groundwaters while some have many times the amount of modern water in them. This
389 likely reflects the fact that inflow groundwater is relic regional groundwater and provides the
390 baseflow to streams in this environment. But some of the streams, particularly the large streams
391 on the Puna plateau are composed of a large amount of recent meteoric water that does not show
392 a strong evaporation signature. The vegas also have a similar signature to these large Puna
393 streams. The other major water groupings display a few distinctive characteristics. Marginal
394 brines and transitional pools plot in a similar position likely reflecting similar sources and
395 interactions between these water bodies. The nucleus brine waters show less evaporation,
396 indicating a distinct combination of sources but skew more towards the regional groundwaters
397 than the marginal water bodies. The lagoon waters tend to fall between the nucleus brines and
398 the marginal/transitional pool waters with a large range of modern components and are less
399 evaporated than the other saline surface waters suggesting they are more closely connected to the
400 inflow waters than other basin floor water bodies.

401 These results reiterate that most inflow is relic water but also show that large streams
402 particularly on the higher elevation plateau can transport substantial volumes of modern water
403 relatively quickly through these systems. These streams along with the vegetated wetland
404 complexes appear to be the primary hydrological conditions under which fresh modern water is
405 captured and transported within human time scales. The fact that the saline basin floor surface
406 water bodies also contain substantial amounts of modern water and that these four water types
407 (streams, vegas, lagoons, and transitional pools) are the only places where water tables exist near
408 the surface in this environment demonstrates this is the primary pathway of modern hydroclimate
409 connection to the larger hydrological cycle. We present the two principle archetypal frameworks
410 that describe these climate-surface water-groundwater interactions in this system.

411 We define the archetypal flow systems in this environment which describe and integrate
412 our observations of transit time and flow paths in the Dry Andes (**Figure 4**). The Ephemeral
413 Surface Flow System is the more common type and is defined by steep topography and structural
414 and hydrogeological conditions that promote infiltration and drop water tables well below the
415 surface (**Figure 4a**). Intermittent streams do often form downgradient of spring complexes in
416 these systems (for example in the southern and eastern parts of the Salar de Atacama and to the
417 east of Salar de Carchi Pampa) but generally flow for short distances downgradient of spring
418 discharge and/or intermittently during large rain events. These streams are fed almost entirely by
419 regional groundwater and contain very small or transitory proportions of modern water. Perched

Figure 4. Conceptual model of archetypal flow regimes in the Dry Andes. Size of the 3H symbol and pie charts show relative modern water content in major water bodies and along flow paths. Arrows show general flow paths from precipitation-to-recharge-to-groundwater colored by relative modern water content from green-to-blue with predicted presence of very old “Fossil” water in teal. Straight arrows show general modern precipitation inputs and regional groundwaters, and zig-zag arrows represent water fluxes to and from the surface scaled by relative flux magnitude. General water body types and geology are colored and textured. (a) Represents the archetype dominated by ephemeral streams and regional groundwater fluxes, (b) represents the archetype dominated by perennial streams that act as efficient conduits for modern water.

420 aquifers do form, in the vicinity of vegetated wetlands at elevation and particularly near the basin
421 floors where the abundance of fine-grained deposits and evaporite precipitation prevents
422 infiltration directly to the deeper water table, these perched aquifers allow moderately aged
423 (years-decades) waters to feed basin floors and importantly create persistent shallow water tables
424 that allow recent rainfall to mix with the saturated zone near the surface. We argue that these
425 conditions are what maintain the vegetated wetlands and lagoons at elevation and allow them to
426 capture and transmit modern precipitation. The dimensions and depth of the water table
427 constitute the dominant control on surface water formation and modern hydroclimate
428 connections in these systems.

429 The other primary archetype in this environment is a perennial surface flow system which
430 is defined primarily by relatively large perennial streams that are also fed predominantly by
431 regional groundwater (baseflow) but maintain consistent flow in all seasons and over large
432 distances (30-100 km) (**Figure 4b**). Smaller topographic gradients and/or hydrological
433 conditions that allow these streams to form create unique hydrological systems that capture more
434 modern rainfall and move it efficiently toward basin floors. The presence of this perennial
435 surface water itself, like shallow water tables, creates conduits that capture modern rainfall and
436 runoff before it evaporates or begins infiltrating through the thick vadose zones. The presence of
437 these conduits is the primary control on connections between the modern hydroclimate and
438 surface waters in these systems. Across most of this arid landscape, when rainfall does occur,
439 much of it rapidly evaporates at the surface and as it makes its way toward the water table, the
440 0.01-5% of that water that reaches the water table as groundwater recharge (now and during past
441 climate conditions) sustains the regional groundwater system (Scanlon et al., 2006; Boutt et al.,
442 2021). These mechanisms are also responsible for maintaining the saline water bodies near the

443 basin floors and on the salars. Groundwater discharge is focused near the basin floor where the
444 topography flattens and fine-grained units have accumulated, creating permeability contrasts that
445 both force water to the surface and restrict infiltration. These conditions create persistent shallow
446 water tables that in turn allow modern waters to efficiently mix with relic groundwaters.

447 **3.4. Implications for society and ecosystems**

448 The extreme decoupling between basin-to-regional scale groundwaters, which constitute
449 the primary inflow to these endorheic basins, and local, modern precipitation inputs has major
450 implications for the management and future sustainability of water systems in the Dry Andes and
451 other arid mountain environments. Our results show that modern precipitation comprises only a
452 small portion of modern hydrological budgets in these environments but is critical to maintaining
453 surface water bodies and vegetation due to a unique but intrinsic set of hydrogeological
454 conditions. The Sixth Assessment Report from the Intergovernmental Panel on Climate Change
455 (IPCC) reports a high confidence projection of increased drought extent and severity in the area
456 (IPCC 2022), which presents threats to the delicate balance of these environments and
457 hydrological systems. Prolonged droughts have been shown to cause major and rapid changes to
458 surface water systems in this region over the last few decades (Frau et al., 2021; Moran et al.,
459 2022). It is critical to understand the current interplay between pre-modern and modern waters to
460 define how human use and changing temperature and precipitation in the region could alter the
461 integrity of these systems. We define the modern and relic water systems in this region for the
462 first time within a framework that reconciles the prevalence of relic groundwater in these
463 environments with the observations of rapid changes to surface waters in response to natural and
464 anthropogenic perturbations.

465 A major focus in these watersheds is the interplay between competing use of water by a
466 variety of riparian stakeholders and the policies and use rights conferred by water managers.
467 Demands for water resources exist from current metal mines and the massive expansion of
468 exploration for lithium among other commodities, indigenous communities, agriculture, as well
469 as the environmental flows required to maintain existing ecosystem services and functions. There
470 is a lack of watershed-specific knowledge of water resources in the region, meaning that water
471 management is naïve to the pre-modern and modern water balance dynamics. If left unfilled, this
472 knowledge gap could lead to use patterns that threaten the viability of these hydrological
473 systems. Moreover, there is limited regional coordination and oversight related to water
474 management in the area which exacerbates the sustainable water management challenge.

475 The work presented in this study provides an important starting point for filling the
476 technical knowledge gap surrounding water balances in these environments. The present work
477 develops a general framework for users of water in these basins and presents the opportunity to
478 revise water budgets within scientifically justifiable frameworks that do not require steady-state
479 closure of basin budgets to allocate water resources more responsibly. In addition, this new
480 understanding can greatly improve our ability to attribute current and future impacts from
481 anthropogenic activities in fragile wetlands systems and predict and respond more effectively to
482 the accelerating impacts of human-induced climate change. This analysis and the new
483 hydrological conceptual models we present will improve our ability to reduce the risk of
484 depleting vulnerable freshwater resources and damaging ecosystems reliant on the delicate
485 balance between modern and pre-modern water inputs and plan human development that avoids
486 the most damaging potential impacts on water quantity and quality. For instance, a particular
487 focus with high potential benefit would be to prioritize the protection of these modern water

488 conduits from disruption or obstruction and/or the removal of existing obstructions. An
489 understanding of connections to modern and past climates will also improve our ability to plan
490 for the effects of future climate changes in these environments.

491 **Data Availability**

492 All data necessary to interpret, replicate, and build upon the findings reported in this article are
493 provided as tables in the supplemental information.

494 **References**

- 495 AghaKouchak, A., Feldman, D., Hoerling, M., Huxman, T. & Lund, J. Water and climate:
496 Recognize anthropogenic drought. *Nature* 524, 409–11 (2015).
- 497 Ashraf, S., Nazemi, A., & AghaKouchak, A. (2021). Anthropogenic drought dominates
498 groundwater depletion in Iran. *Scientific Reports*, 11(1), 9135.
499 <https://doi.org/10.1038/s41598-021-88522-y>
- 500 Basaldúa, A., Alcaraz, E., Quiroz-Londoño, M., Dapeña, C., Ibarra, E., Vélez-Agudelo, C., ...
501 Martínez, D. (2022). Reconstruction of the record of tritium in precipitation in the
502 temperate zone of South America. *Hydrological Processes*, 36(9), 1–11.
503 <https://doi.org/10.1002/hyp.14691>
- 504 van Beek, L. P. H., Wada, Y., & Bierkens, M. F. P. (2011). Global monthly water stress: 1.
505 Water balance and water availability. *Water Resources Research*, 47(7), n/a-n/a.
506 <https://doi.org/10.1029/2010WR009791>
- 507 Belcher, W. R., Bedinger, M. S., Back, J. T., & Sweetkind, D. S. (2009). Interbasin flow in the
508 Great Basin with special reference to the southern Funeral Mountains and the source of
509 Furnace Creek springs, Death Valley, California, U.S. *Journal of Hydrology*, 369(1–2),
510 30–43. <https://doi.org/10.1016/j.jhydrol.2009.02.048>
- 511 Beria, H., Larsen, J. R., Ceperley, N. C., Michelon, A., Vennemann, T., & Schaepli, B. (2018).
512 Understanding snow hydrological processes through the lens of stable water isotopes.
513 *Wiley Interdisciplinary Reviews: Water*, (June), e1311.
514 <https://doi.org/10.1002/wat2.1311>
- 515 Bierkens, M. F. P., & Wada, Y. (2019). Non-renewable groundwater use and groundwater
516 depletion: a review. *Environmental Research Letters*, 14(6), 063002.
517 <https://doi.org/10.1088/1748-9326/ab1a5f>
- 518 Birkel, C., & Soulsby, C. (2015). Advancing tracer-aided rainfall-runoff modelling: a review of
519 progress, problems and unrealised potential. *Hydrological Processes*, 29(25), 5227–5240.
520 <https://doi.org/10.1002/hyp.10594>

- 521 Boutt, D. F., Hynek, S. A., Munk, L. A., & Corenthal, L. G. (2016). Rapid recharge of fresh
522 water to the halite-hosted brine aquifer of Salar de Atacama, Chile. *Hydrological*
523 *Processes*, 30(25), 4720–4740. <https://doi.org/10.1002/hyp.10994>
- 524 Boutt, D.F., Corenthal, L.G., Moran, B.J. et al. Imbalance in the modern hydrologic budget of
525 topographic catchments along the western slope of the Andes (21–25°S): implications for
526 groundwater recharge assessment. *Hydrogeol J* 29, 985–1007 (2021).
527 <https://doi.org/10.1007/s10040-021-02309-z>
- 528 Buttle, J.M. (1994). Isotope hydrograph separations and rapid delivery of pre-event water from
529 basins drainage. *Phys. Geogr.* 18, 16–41.
- 530 Cartwright, I., Cendón, D., Currell, M., & Meredith, K. (2017). A review of radioactive isotopes
531 and other residence time tracers in understanding groundwater recharge: Possibilities,
532 challenges, and limitations. *Journal of Hydrology*, 555, 797–811.
533 <https://doi.org/10.1016/j.jhydrol.2017.10.053>
- 534 Clark, I. & Fritz, P. (1997). *Environmental Isotopes in Hydrogeology*. Lewis Publications, Boca
535 Raton, FL.
- 536 Clarke, W.B., Jenkins, W.J., Top, Z. (1976). Determination of tritium by mass spectrometric
537 measurement of ^3He . *Int. J. Appl. Radiat. Isot.* 27 (9), 515e522.
- 538 Cook, P.G. and Bohlke, J.K. (2000). Determining timescales for groundwater flow and solute
539 transport. In: Cook, P.G., Herczeg, A.L. (Eds.), *Environmental Tracers in Subsurface*
540 *Hydrology*. Kluwer, Boston, pp. 1–30.
- 541 Corenthal, L. G., D. F. Boutt, S. A. Hynek, and L. A. Munk (2016), Regional groundwater flow
542 and accumulation of a massive evaporite deposit at the margin of the Chilean Altiplano,
543 *Geophys. Res. Lett.*, 43, doi:10.1002/2016GL070076
- 544 Cortecchi, G., Boschetti, T., Mussi, M., Lameli, C. H., Mucchino, C., & Barbieri, M. (2005). New
545 chemical and original isotopic data on waters from El Tatio geothermal field, northern
546 Chile. *Geochemical Journal*, 39(6), 547–571. <https://doi.org/10.2343/geochemj.39.547>
- 547 Crawford, Alec Lunde Seefeldt, Jennapher, Kent, Richard, Helbert, Maryse, Pimentel, Guzmán,
548 Gonzalo, González, Alejandro, Chen, Zheng, and Andy Abbott. (2021) Lithium: The big
549 picture. *One Earth* 4(3): 323-326. <https://doi.org/10.1016/j.oneear.2021.02.021>
- 550 Dansgaard, W. (1964), Stable isotopes in precipitation, *Tellus*, 16(4), 436–468,
551 doi:10.1111/j.2153-3490.1964.tb00181.x.
- 552 Díaz Paz, Walter Fernando., Escosteguy, Melisa., Seghezze, Lucas., Hufty, Marc., Kruse,
553 Eduardo., and Martín Alejandro Iribarnegaray, (2023). Lithium mining, water resources,
554 and socio-economic issues in northern Argentina: We are not all in the same boat.
555 *Resources Policy* 81 (2023): 103288, <https://doi.org/10.1016/j.resourpol.2022.103288>
- 556 Favreau, G., Cappelaere, B., Massuel, S., Leblanc, M., Boucher, M., Boulain, N., & Leduc, C.
557 (2009). Land clearing, climate variability, and water resources increase in semiarid
558 southwest Niger: A review. *Water Resources Research*, 45(7), 1–18.
559 <https://doi.org/10.1029/2007WR006785>

- 560 Fan, Y., Li, H., & Miguez-Macho, G. (2013). Global Patterns of Groundwater Table Depth.
561 *Science*, 339(6122), 940–943. <https://doi.org/10.1126/science.1229881>
- 562 Frau, D., Moran, B. J., Arengo, F., Marconi, P., Battauz, Y., Mora, C., ... Boutt, D. F. (2021).
563 Hydroclimatological Patterns and Limnological Characteristics of Unique Wetland
564 Systems on the Argentine High Andean Plateau. *Hydrology*, 8(4), 164.
565 <https://doi.org/10.3390/hydrology8040164>
- 566 Gamboa, C., Godfrey, L., Herrera, C., Custodio, E., & Soler, A. (2019). The origin of solutes in
567 groundwater in a hyper-arid environment: A chemical and multi-isotope approach in the
568 Atacama Desert, Chile. *Science of The Total Environment*, 690, 329–351.
569 <https://doi.org/10.1016/j.scitotenv.2019.06.356>
- 570 Gajardo, G., & Redón, S. (2019). Andean hypersaline lakes in the Atacama Desert, northern
571 Chile: Between lithium exploitation and unique biodiversity conservation. *Conservation
572 Science and Practice*, 1(9), 1–8. <https://doi.org/10.1111/csp2.94>
- 573 Gayo, E. M., C. Latorre, T. E. Jordan, P. L. Nester, S. A. Estay, K. F. Ojeda, and C. M. Santoro
574 (2012), Late Quaternary hydrological and ecological changes in the hyperarid core of the
575 northern Atacama Desert (~21°S), *Earth-Science Rev.*, 113(3-4), 120–140,
576 [doi:10.1016/j.earscirev.2012.04.003](https://doi.org/10.1016/j.earscirev.2012.04.003).
- 577 Ge, J., Chen, J., Ge, L., Wang, T., Wang, C., & Chen, Y. (2016). Isotopic and hydrochemical
578 evidence of groundwater recharge in the Hopq Desert, NW China. *Journal of
579 Radioanalytical and Nuclear Chemistry*, 310(2), 761–775.
580 <https://doi.org/10.1007/s10967-016-4856-8>
- 581 Gleeson, T., L. Marklund, L. Smith, and A. H. Manning (2011), Classifying the water table at
582 regional to continental scales, *Geophys. Res. Lett.*, 38(5), 1–6,
583 [doi:10.1029/2010GL046427](https://doi.org/10.1029/2010GL046427)
- 584 Gleeson, T., Wada, Y., Bierkens, M. F. P., & van Beek, L. P. H. (2012). Water balance of global
585 aquifers revealed by groundwater footprint. *Nature*, 488(7410), 197–200.
586 <https://doi.org/10.1038/nature11295>
- 587 Gleeson, T. (2020). Global Groundwater Sustainability. *Groundwater*, 58(4), 484–485.
588 <https://doi.org/10.1111/gwat.12991>
- 589 Godfrey, L. V., Chan, L.-H., Alonso, R. N., Lowenstein, T. K., McDonough, W. F., Houston, J.,
590 ... Jordan, T. E. (2013). The role of climate in the accumulation of lithium-rich brine in
591 the Central Andes. *Applied Geochemistry*, 38, 92–102.
592 <https://doi.org/10.1016/j.apgeochem.2013.09.002>
- 593 Grosjean, Martin; Geyh, Mebus A.; Messerli, Bruno; Schotterer, U. (1995). Late-glacial and
594 early Holocene lake sediments, groundwater formation and climate in the Atacama
595 Altiplano 22-24°S. *Journal of Paleolimnology*, 14, 241–252.
- 596 Gutiérrez, J. S., Navedo, J. G., & Soriano-Redondo, A. (2018). Chilean Atacama site imperilled
597 by lithium mining. *Nature*, 557(7706), 492–492. <https://doi.org/10.1038/d41586-018-05233-7>
598

- 599 Hartley, A. J., and G. Chong (2002), Late Pliocene age for the Atacama Desert: Implications for
600 the desertification of western South America, *Geology*, 30(1), 43–46, doi:10.1130/0091-
601 7613(2002)030<0043:LPAFTA>2.0.CO;2.
- 602 Haitjema, H. M., and S. Mitchell-Bruker (2005), Are Water Tables a Subdued Replica of the
603 Topography?, *Ground Water*, 43(6), 781–786, doi:10.1111/j.1745-6584.2005.00090.x.
- 604 Herrera, C., Custodio, E., Chong, G., Lambán, L. J., Riquelme, R., Wilke, H., ... Lictevoud, E.
605 (2016). Groundwater flow in a closed basin with a saline shallow lake in a volcanic area:
606 Laguna Tuyajto, northern Chilean Altiplano of the Andes. *Science of The Total*
607 *Environment*, 541, 303–318. <https://doi.org/10.1016/j.scitotenv.2015.09.060>
- 608 Houston, J. (2002). Groundwater recharge through an alluvial fan in the Atacama Desert,
609 northern Chile: mechanisms, magnitudes and causes. *Hydrological Processes*, 16(15),
610 3019–3035. <https://doi.org/10.1002/hyp.1086>
- 611 Houston, J. (2007). Recharge to groundwater in the Turi Basin, northern Chile: An evaluation
612 based on tritium and chloride mass balance techniques. *Journal of Hydrology*, 334(3–4),
613 534–544. <https://doi.org/10.1016/j.jhydrol.2006.10.030>
- 614 Houston, J. (2009). A recharge model for high altitude, arid, Andean aquifers. *Hydrological*
615 *Processes*, 23(16), 2383–2393. <https://doi.org/10.1002/hyp.7350>
- 616 Immerzeel, W. W., Lutz, A. F., Andrade, M., Bahl, A., Biemans, H., Bolch, T., ... Baillie, J. E.
617 M. (2020). Importance and vulnerability of the world's water towers. *Nature*, 577(7790),
618 364–369. <https://doi.org/10.1038/s41586-019-1822-y>
- 619 IPCC, 2022: Climate Change 2022: Impacts, Adaptation, and Vulnerability. Contribution of
620 Working Group II to the Sixth Assessment Report of the Intergovernmental Panel on
621 Climate Change [H.-O. Pörtner, D.C. Roberts, M. Tignor, E.S. Poloczanska, K.
622 Mintenbeck, A. Alegría, M. Craig, S. Langsdorf, S. Löschke, V. Möller, A. Okem, B.
623 Rama (eds.)]. Cambridge University Press. Cambridge University Press, Cambridge, UK
624 and New York, NY, USA, 3056 pp., doi:10.1017/9781009325844.
- 625 Jasechko, S. (2016). Partitioning young and old groundwater with geochemical tracers. *Chemical*
626 *Geology*, 427, 35–42. <https://doi.org/10.1016/j.chemgeo.2016.02.012>
- 627 Jordan, T., Lameli, C. H., Kirk-Lawlor, N., & Godfrey, L. (2015). Architecture of the aquifers of
628 the Calama Basin, Loa catchment basin, northern Chile. *Geosphere*, 11(5), 1438–1474.
629 <https://doi.org/10.1130/GES01176.1>
- 630 Kendall, C. & Caldwell, E.A. (1998) Fundamentals of isotope geochemistry. In: *Isotope Tracers*
631 *in Catchment Hydrology* (Eds C. Kendall & J.J. McDonnell), pp. 51-86. Elsevier,
632 Amsterdam.
- 633 Kendall, C., McDonnell, J.J. (1998). *Isotope Tracers in Catchment Hydrology*. 839 pp. Elsevier,
634 New York
- 635 Kroepelin, S., Verschuren, D., Lezine, A.-M., Eggermont, H., Cocquyt, C., Francus, P., ...
636 Engstrom, D. R. (2008). Climate-Driven Ecosystem Succession in the Sahara: The Past
637 6000 Years. *Science*, 320(5877), 765–768. <https://doi.org/10.1126/science.1154913>

- 638 Liu, Y., Wagener, T., Beck, H. E., & Hartmann, A. (2020). What is the hydrologically effective
639 area of a catchment? *Environmental Research Letters*, 15(10), 104024.
640 <https://doi.org/10.1088/1748-9326/aba7e5>
- 641 Lucas, L., & Unterweger, M. (2000). Comprehensive review and critical evaluation of the half-
642 life of tritium. *Journal of Research of the National Institute of Standards and Technology*,
643 105(4), 541–549. <https://doi.org/10.6028/jres.105.043>
- 644 Masbruch, M. D., Rumsey, C. A., Gangopadhyay, S., Susong, D. D., & Pruitt, T. (2016).
645 Analyses of infrequent (quasi-decadal) large groundwater recharge events in the northern
646 Great Basin: Their importance for groundwater availability, use, and management. *Water*
647 *Resources Research*, 52(10), 7819–7836. <https://doi.org/10.1002/2016WR019060>
- 648 Marconi, P., Arengo, F., & Clark, A. (2022). The arid Andean plateau waterscapes and the
649 lithium triangle: flamingos as flagships for conservation of high-altitude wetlands under
650 pressure from mining development. *Wetlands Ecology and Management*, (0123456789).
651 <https://doi.org/10.1007/s11273-022-09872-6>
- 652 McKnight, S. V., Boutt, D. F., & Munk, L. A. (2021). Impact of Hydrostratigraphic Continuity
653 on Brine-to-Freshwater Interface Dynamics: Implications From a Two-Dimensional
654 Parametric Study in an Arid and Endorheic Basin. *Water Resources Research*, 57(4).
655 <https://doi.org/10.1029/2020WR028302>
- 656 McKnight, S. V., Boutt, D. F., Munk, L. A., & Moran, B. (2023). Distinct Hydrologic Pathways
657 Regulate Perennial Surface Water Dynamics in a Hyperarid Basin. *Water Resources*
658 *Research*, 59(4). <https://doi.org/10.1029/2022WR034046>
- 659 Mehran, A., Mazdiyasn, O. & AghaKouchak, A. A hybrid framework for assessing
660 socioeconomic drought: Linking climate variability, local resilience, and demand. *J.*
661 *Geophys. Res. Atmos.* 120, 7520–7533 (2015)
- 662 Mehran, A., AghaKouchak, A., Nakhjiri, N. et al. Compounding Impacts of Human-Induced
663 Water Stress and Climate Change on Water Availability. *Sci Rep* 7, 6282 (2017).
664 <https://doi.org/10.1038/s41598-017-06765-0>
- 665 Moran, B. J., Boutt, D. F., & Munk, L. A. (2019). Stable and Radioisotope Systematics Reveal
666 Fossil Water as Fundamental Characteristic of Arid Orogenic-Scale Groundwater
667 Systems. *Water Resources Research*, 55(12), 11295–11315.
668 <https://doi.org/10.1029/2019WR026386>
- 669 Moran, Brendan J.; Boutt, David F.; McKnight, Sarah V.; Jenckes, Jordan; Munk, Lee Ann;
670 Corkran, Daniel; and Kirshen, Alexander, "Data for "Relic Groundwater and Mega
671 Drought Confound Interpretations of Water Sustainability and Lithium Extraction in Arid
672 Lands"" (2021). Data and Datasets. 145. <https://scholarworks.umass.edu/data/145>
- 673 Munk, L.A., Hynek, S.A., Bradley, D.C., Boutt, D.F., Labay, K., Jochens, H., (2016). Lithium
674 Brines: A Global Perspective, in Verplanck, P.L. and Hitzman, M.W., eds., *Rare Earth*
675 *and Critical Elements in Ore Deposits. Reviews in Economic Geology* (18), 339–365.
- 676 Munk, L. A., Boutt, D. F., Hynek, S. A., & Moran, B. J. (2018). Hydrogeochemical fluxes and
677 processes contributing to the formation of lithium-enriched brines in a hyper-arid

- 678 continental basin. *Chemical Geology*, 493, 37–57.
679 <https://doi.org/10.1016/j.chemgeo.2018.05.013>
- 680 Munk, L. A., Boutt, D. F., Moran, B. J., McKnight, S. V., & Jenckes, J. (2021). Hydrogeologic
681 and geochemical distinctions in freshwater-brine systems of an Andean salar.
682 *Geochemistry, Geophysics, Geosystems*, 22, e2020GC009345.
683 <https://doi.org/10.1029/2020GC009345>
- 684 Panichi C. and Gonfiantini R.. Environmental isotopes in geothermal studies. *Geothermics*
685 1977;6(3-4):143-161. [https://doi.org/10.1016/0375-6505\(77\)90024-4](https://doi.org/10.1016/0375-6505(77)90024-4)
- 686 Pfeiffer, M., Latorre, C., Santoro, C. M., Gayo, E. M., Rojas, R., Carrevedo, M. L., ...
687 Amundson, R. (2018). Chronology, stratigraphy and hydrological modelling of extensive
688 wetlands and paleolakes in the hyperarid core of the Atacama Desert during the late
689 quaternary. *Quaternary Science Reviews*, 197, 224–245.
690 <https://doi.org/10.1016/j.quascirev.2018.08.001>
- 691 Placzek, C. J., J. Quade, and P. J. Patchett (2013), A 130ka reconstruction of rainfall on the
692 Bolivian Altiplano, *Earth Planet. Sci. Lett.*, 363, 97–108, doi:10.1016/j.epsl.2012.12.017.
- 693 Rech, J. A., Currie, B. S., Jordan, T. E., Riquelme, R., Lehmann, S. B., Kirk-Lawlor, N. E., ...
694 Gooley, J. T. (2019). Massive middle Miocene gypsic paleosols in the Atacama Desert
695 and the formation of the Central Andean rain-shadow. *Earth and Planetary Science*
696 *Letters*, 506, 184–194. <https://doi.org/10.1016/j.epsl.2018.10.040>
- 697 Rissmann, C., Leybourne, M., Benn, C., & Christenson, B. (2015). The origin of solutes within
698 the groundwaters of a high Andean aquifer. *Chemical Geology*, 396, 164–181.
699 <https://doi.org/10.1016/j.chemgeo.2014.11.029>
- 700 Rooyen, J. D., Watson, A. P., Palcsu, L., & Miller, J. A. (2021). Constraining the Spatial
701 Distribution of Tritium in Groundwater Across South Africa. *Water Resources Research*,
702 57(8). <https://doi.org/10.1029/2020WR028985>
- 703 Scanlon, B. R., Keese, K. E., Flint, A. L., Flint, L. E., Gaye, C. B., Edmunds, W. M., &
704 Simmers, I. (2006). Global synthesis of groundwater recharge in semiarid and arid
705 regions. *Hydrological Processes*, 20(15), 3335–3370. <https://doi.org/10.1002/hyp.6335>
- 706 Scheihing, K. W., Moya, C. E., Struck, U., Lictevout, E., & Tröger, U. (2018). Reassessing
707 hydrological processes that control stable Isotope Tracers in groundwater of the Atacama
708 Desert (Northern Chile). *Hydrology*, 5(1). <https://doi.org/10.3390/hydrology5010003>.
- 709 Somers, L. D., & McKenzie, J. M. (2020). A review of groundwater in high mountain
710 environments. *WIREs Water*, 7(6). <https://doi.org/10.1002/wat2.1475>
- 711 Sonter, L. J., Dade, M. C., Watson, J. E. M., & Valenta, R. K. (2020). Renewable energy
712 production will exacerbate mining threats to biodiversity. *Nature Communications*, 11(1),
713 4174. <https://doi.org/10.1038/s41467-020-17928-5>
- 714 Stewart, M. K., Morgenstern, U., Gusyev, M. A., & Maloszewski, P. (2017). Aggregation effects
715 on tritium-based mean transit times and young water fractions in spatially heterogeneous
716 catchments and groundwater systems, and implications for past and future applications of

- 717 tritium. *Hydrology and Earth System Sciences Discussions*, (October), 1–26.
718 <https://doi.org/10.5194/hess-2016-532>
- 719 Viguier, B., Jourde, H., Leonardi, V., Lictévout, E., & Daniele, L. (2020). Water table variations
720 in Atacama desert alluvial fans: Discussion of “evidence of short-term groundwater
721 recharge signal propagation from the Andes to the central Atacama desert: A singular
722 spectrum analysis approach.” *Hydrological Sciences Journal*, 65(9), 1606–1613.
723 <https://doi.org/10.1080/02626667.2020.1764001>
- 724 Walvoord, M. A., Plummer, M. A., Phillips, F. M., & Wolfsberg, A. V. (2002). Deep arid system
725 hydrodynamics 1. Equilibrium states and response times in thick desert vadose zones.
726 *Water Resources Research*, 38(12), 44-1-44–15. <https://doi.org/10.1029/2001WR000824>
- 727 Wang, J., Song, C., Reager, J. T., Yao, F., Famiglietti, J. S., Sheng, Y., ... Wada, Y. (2018).
728 Recent global decline in endorheic basin water storages. *Nature Geoscience*, 11(12), 926–
729 932. <https://doi.org/10.1038/s41561-018-0265-7>
- 730 Wheeler, H., Sorooshian, S., & Sharma, K. (Eds.). (2007). *Hydrological Modelling in Arid and*
731 *Semi-Arid Areas (International Hydrology Series)*. Cambridge: Cambridge University
732 Press. doi:10.1017/CBO9780511535734
- 733 Wood, C., Cook, P. G., & Harrington, G. A. (2015). Vertical carbon-14 profiles for resolving
734 spatial variability in recharge in arid environments. *Journal of Hydrology*, 520, 134–142.
735 <https://doi.org/10.1016/j.jhydrol.2014.11.044>
- 736 Zipper, S. C., Jaramillo, F., Wang-Erlandsson, L., Cornell, S. E., Gleeson, T., Porkka, M., ...
737 Gordon, L. (2020). Integrating the Water Planetary Boundary With Water Management
738 From Local to Global Scales. *Earth’s Future*, 8(2).
739 <https://doi.org/10.1029/2019EF001377>

740 **Acknowledgments**

741 The authors would like to thank Felicity Arengo, Patricia Marconi, and Diego Frau for inviting
742 us to join multiple sampling campaigns that were pivotal to collecting the data that initiated this
743 study on the Puna. We also want to thank Ricki Sheldon, the Consejo de Pueblos Atacameños,
744 Asociación de Agricultores Zapar, Asociación de Agricultores Soncor, Comunidad de Toconao,
745 Comunidad de Catarpe, Comunidad de Coyo, Familia Bautista de Tambillo, and CONAF for
746 graciously volunteering to access and conduct sampling that was pivotal to this study.

747 **Author Contributions**

748 Conceptualization, B.M; Methodology, B.M., D.B; Formal Analysis, B.M.; Investigation, B.M.,
749 D.B., L.M.; Resources, D.B., L.M., J.F.; Writing – Original Draft Preparation, B.M.; Writing –
750 Review & Editing, B.M., D.B., L.M., J.F.; Funding Acquisition, B.M., D.B., L.M., J.F.

751

752 **Competing Interests**

753 The authors declare no competing interests.

754 **Supplementary Information**

755 Included in a separate document with this submission.

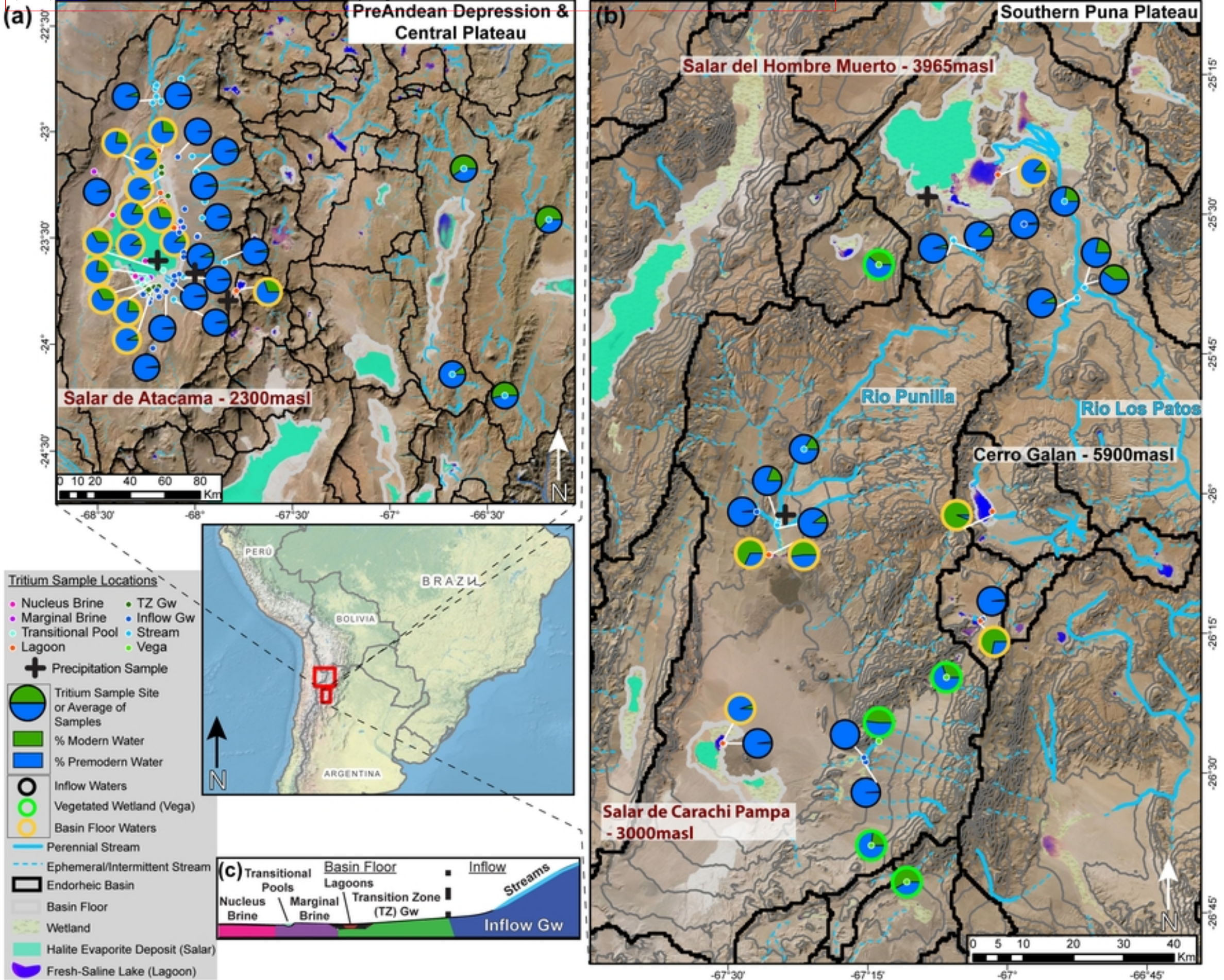


Figure 1

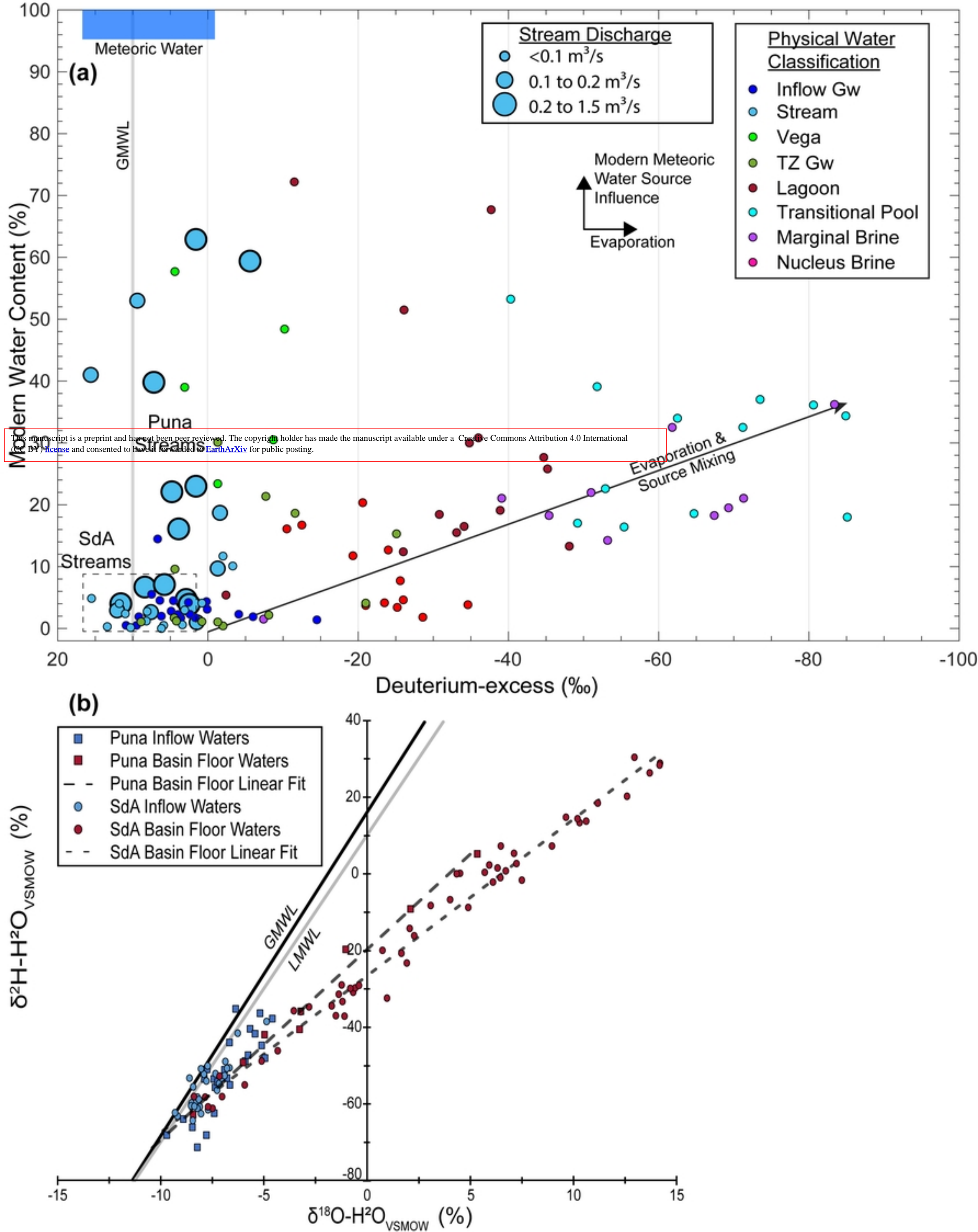


Figure 3

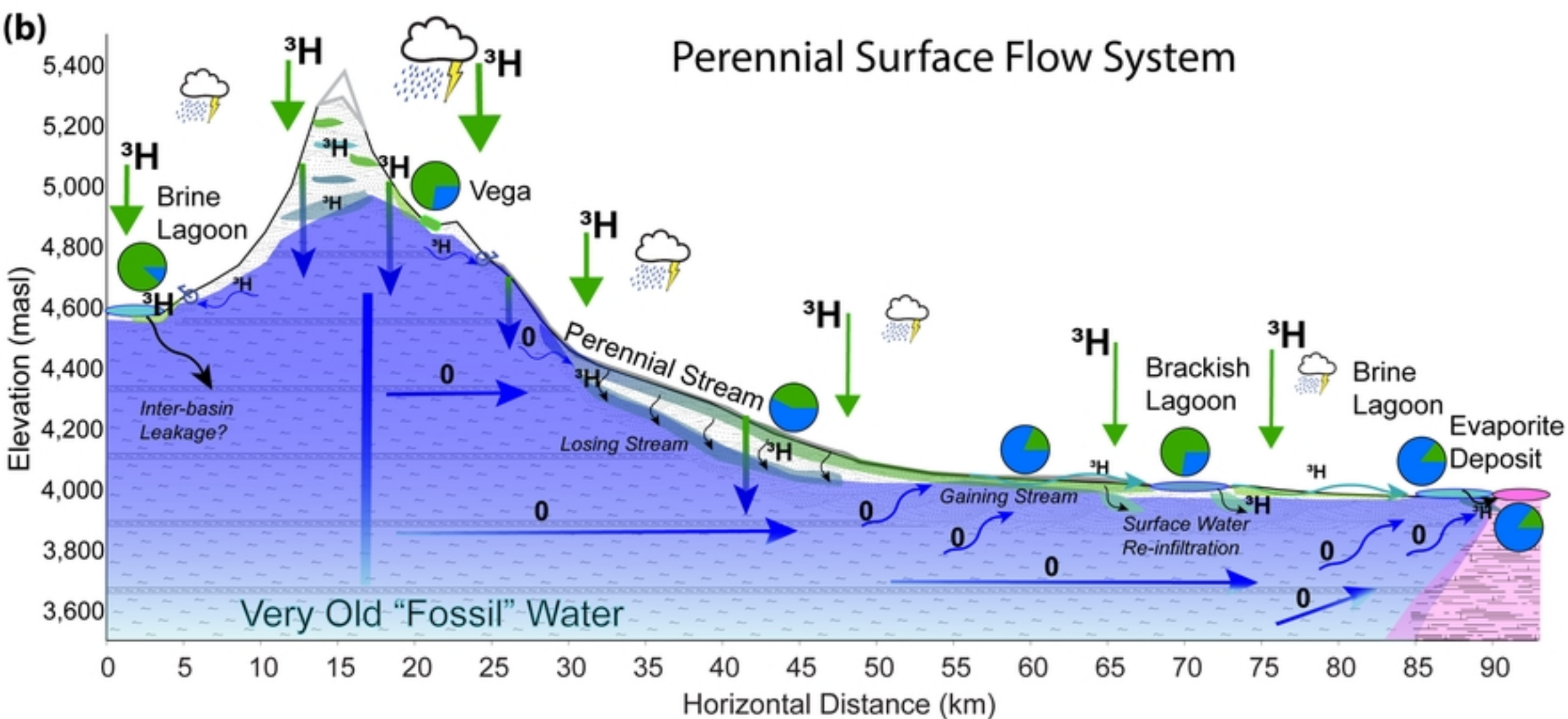
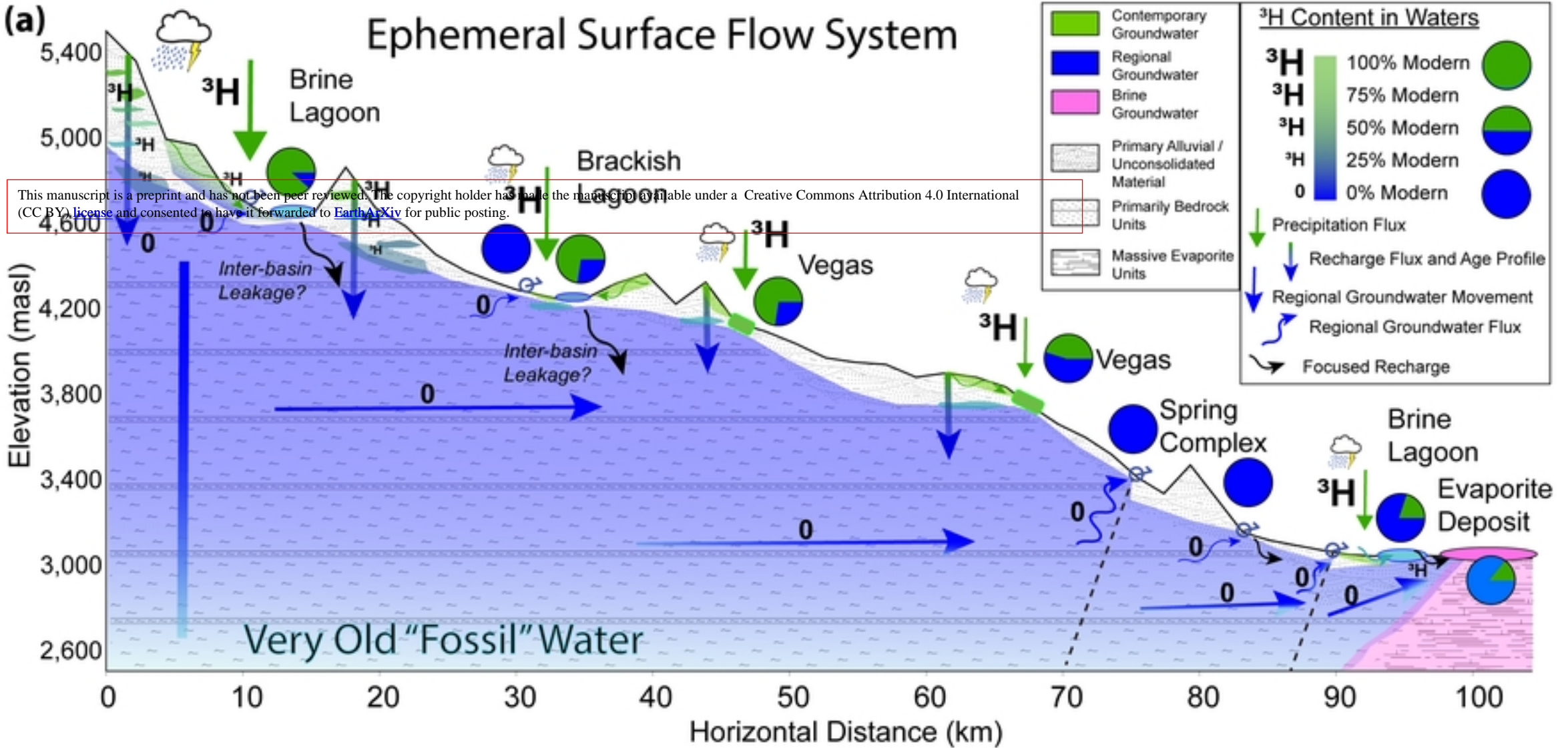


Figure 4

